An Experimental Study on Indoor Massive 3D-MIMO Channel at 30-40 GHz Band

Citation for the original published paper (version of record):

(article starts on next page)

An Experimental Study on Indoor Massive 3D-MIMO Channel at 30-40 GHz Band

Jiliang Zhang[1], Andrés Alayón Glazunov[1,2], Jian Yang[1], Xiaoli Chu[3], and Jie Zhang[3]

1 Department of Electrical Engineering, Chalmers University of Technology, Gothenburg, SE
2 Department of Electrical Engineering, University of Twente, Enschede, Overijssel, NL
3 Department of Electronic and Electrical Engineering, University of Sheffield, Sheffield, UK

Abstract - **Three-dimensional (3D) multiple-input multiple-output (MIMO) channel sounder measurements of a multi-user MIMO channel at the 30-40 GHz mm-wave band are presented. 3D-MIMO downlink transmissions to two users is considered. The measurement campaign employing a vector network analyzer (VNA) has been performed in an office scenario. The mm-wave 3D-MIMO channel is characterized in the wavenumber domain and the time domain via a 3D inverse fast Fourier transform (IFFT). It is shown that the massive 3D-MIMO significantly improve the estimation resolution of multipath components as compared to none-massive 3D-MIMO.**

Index Terms — **mm-wave, 3D-MIMO, massive MIMO, channel sounding, radio propagation.**

1. Introduction

The large number of degrees of freedom (DoF) in the space domain due to the large number of antennas and the large available bandwidth at the millimeter wave (mm-wave) band makes the massive 3D multi-user (MU) multiple-input multiple-output (MIMO) a promising technology for 5G mobile networks [1,2]. The measurement-based channel modelling becomes therefore critical for mm-wave 3D-MIMO system design and network optimization [3].

Accurate channel sounder measurements are required to spatially characterize the 3D-MIMO channel. The vector network analyzer (VNA) offers a large MIMO measurement bandwidth [4,5]. Virtual array antenna systems can be produced with VNA channel sounding techniques without using expensive large array antennas [6].

In this paper, we report VNA based downlink mm-wave 3D-MIMO channel sounder measurements with a virtual uniform rectangular array (URA) of 256 (16 × 16) antenna elements. The measurement campaign involving transmissions to two users was conducted in an office scenario. The measured channel impulse responses are analyzed in the wavenumber domain and the time domain. Measurement shows that the massive 3D-MIMO with a 16 × 16 URA provides a much better resolution of multipath components than that with a 4 × 4 URA.

2. Channel Sounder

The 3D-MIMO channel sounder employing the Agilent VNA E8363 is shown in Fig. 1. The measurements were carried out at a center frequency f_c = 35 GHz with a bandwidth of 10 GHz. Thus, the delay resolution is 0.1 ns.
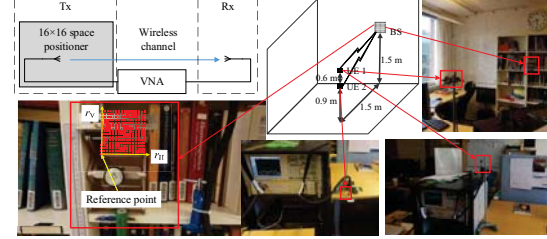

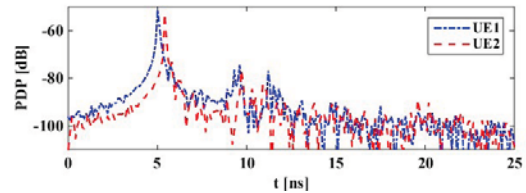Fig. 1. The channel sounder and the measurement scenario.

Fig. 2. The measured power density profile.

Two open waveguide antennas were employed to transmit and receive radio frequency signals. At the base station (BS) end, the transmit antenna is moved within a fixed grid of 16 × 16 points with a spatial interval of 5 mm that provides a virtual uniform rectangular array (URA) antenna. At the user equipment (UE) end, a single-element receive antenna is used. The VNA measures the $S_{21}(\boldsymbol{\omega}, \boldsymbol{r}_V, \boldsymbol{r}_H)$ of the wireless channel, where $\boldsymbol{\omega}$ is a vector of angular frequency samples with N_f elements, $\boldsymbol{r}_V$ and $\boldsymbol{r}_H$ are vectors of transmit element positions relative to the reference pint of the virtual-array. The number of measured frequency points N_f = 1601, i.e., $\boldsymbol{\omega}$ = 2π × [30, 30.00625, 30.0125, ..., 39.99375, 40] × 10^9 Grads/s. For the 16 × 16 virtual transmit array, $\boldsymbol{r}_V = \boldsymbol{r}_H$ = [0, 5, 10, ..., 75] mm. A laptop is used to collect and analyze the data from the VNA.

3. Measurement Setup

The measurement was carried out in an office room in Hörsalsvägen 11, ED-building, floor 7, Chalmers University of Technology, as shown in Fig. 1. The virtual BS URA was located on the shelf. Two UEs, which are denoted as UE1 and UE2, respectively, were located at 1.5 m distance from the BS. The transmissions from the BS to both UEs are in line of sight (LOS). Before carrying out the measurements, the whole system was calibrated using the VNA. During the measurements, there were no moving scatterers indoors and the measured channel was static.
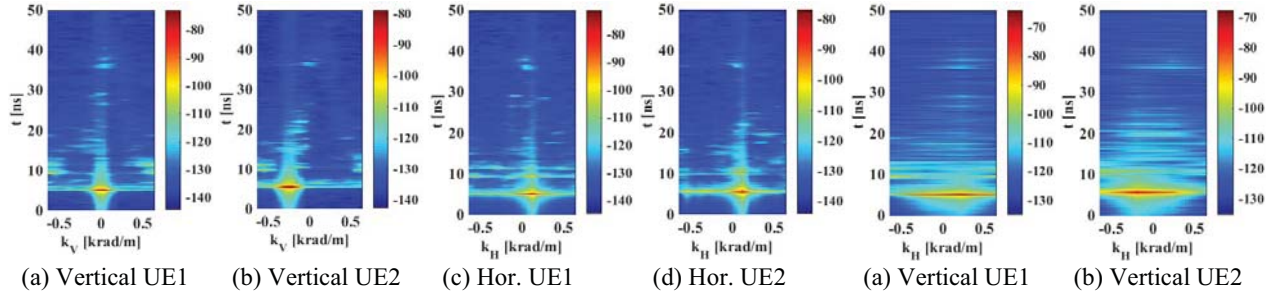
(a) Vertical UE1   (b) Vertical UE2   (c) Hor. UE1   (d) Hor. UE2   (a) Vertical UE1   (b) Vertical UE2

Fig. 3. The delay-wavenumber profile for 16 × 16 URA.   Fig. 4. The delay-wavenumber profile for 4 × 4 URA.

4. Measurement results and analysis

The power delay profile (PDP) is computed from the measured data by

$$P_{DP}(t) = E_{r_V, r_H}\left[\left|h(t, r_V, r_H)\right|^2\right], \tag{1}$$

where $h(t, r_V, r_H)$ is the channel impulse response (CIR) computed by inverse fast Fourier transform (IFFT) of the $S_{21}(\omega, r_V, r_H)$. The PDPs for the UE1 and UE2 are shown in Fig. 2. As can be seen, multipath components with a path length difference less than 3 cm can be distinguished well due to a delay resolution of 0.1 ns. It is observed that the power of non-LOS multipath components is 25 dB below the LOS level at 30-40 GHz due to the high directivity of the antennas. Even with a massive MIMO at BS, both UEs has two major common multipath components with delays of around 9 ns and 11 ns, respectively.

The delay-wavenumber function is computed by

$$F_{DWP}(t, k_V, k_H) = \text{IFFT3}\left[S_{21}(\omega, r_V, r_H)\right], \tag{2}$$

where the IFFT3 is the 3D inverse fast Fourier transform, which is equivalent to computing the 1-D transform along ω, r_V, and r_H, independently. The vectors k_V and k_H denote wavenumbers of multipaths in the vertical and the horizontal directions, respectively. The IFFT from r_V and r_H to k_V and k_H holds because the wavenumber domain can be considered as the spectral domain of position [Table 2.2, 7]. In the space domain, a Hamming window is used to reduce the power of the side lobes in the wavenumber domain. The aperture of the URA is 7.5 mm × 7.5 mm, and the resolution of the wavenumber domain is 83.8 rad/m × 83.8 rad/m. (k_V, k_H) is a bijection of the angles of arrival (AOA) (θ, ϕ). More specifically, for any (θ, ϕ), we have

$$k_V = \frac{2\pi\sin\theta\cos\phi}{\lambda}, \tag{3}$$

$$k_H = \frac{2\pi\sin\theta\sin\phi}{\lambda}. \tag{4}$$

Fig. 3 shows the delay-wavenumber functions for the UE1 and UE2. For t, k_V, or k_H, the mm-wave channels behave as a combination of a few resolvable multi-paths. From Fig. 3(c-d), we found that the both users are not easy to be distinguished in the horizontal delay-wavenumber profiles. The similarity of the horizontal delay-wavenumber profiles leads to the worse performance of the traditional 2D-MU-MIMO. Fortunately, the two UEs are more distinguishable in the vertical delay-wavenumber profiles, see Fig. 3(a-b), since

the elevation wave number profiles of UEs show a larger difference. Hence, in this typical indoor scenario, using the 3D-MU-MIMO to carry out beamforming is feasible. Moreover, the advantage of 3D-MIMO arises with the implementation of massive MIMO array antennas. For comparison, the delay-wavenumber profile for the wireless channel with a 4 × 4 URA is shown in Fig. 4. The lower resolution in the wavenumber domain, i.e., 419 rad/m × 419 rad/m, may therefore have a detrimental impact on the performance of 3D MIMO.

5. Conclusions

An indoor 3D-MIMO channel with two users was measured and analyzed. The URA with 256 elements provides high wavenumber resolution in both vertical and horizontal directions. The analysis shows that the spatial resolution of 3D-MIMO relies on the size of the antenna array. In the future, we will design an accurate 3D automatic space positioner and carry out comprehensive channel measurement.

Acknowledgment

References

[1]   J. G. Andrews et al., "What will 5G be?" *IEEE J. Sel. Areas Commun.*, vol. 32, no. 6, pp. 1065-1082, 2014.

[2]   X. Cheng et al., "Communicating in the real world: 3D MIMO," *IEEE Wireless Commun.*, vol. 21, no. 4, pp. 136-144, 2014.

[3]   J. Zhang et al., "Three-dimensional fading channel models: A survey of elevation angle research," *IEEE Commun. Mag.*, vol. 52, no. 6, pp. 218-226, 2014.

[4]   J. Zhang et al., "Bit error probability of spatial modulation over measured indoor channels," *IEEE Trans Wireless Commun.*, vol. 13, no. 3, pp. 1380-1387.

[5]   L. Hu et al., "Spatial characterization of indoor MIMO radio channel at both 6.05GHz and 2.45GHz based on measurement," *IEEE WCSP*, 2015

[6]   A. W. Mbugua et al., "Millimeter wave multi-user performance evaluation based on measured channels with virtual antenna array channel sounder," *IEEE Access*, vol. 6, pp. 12318-12326, 2018.

[7]   G. D. Durgin, "Space-time wireless channels," *Prentice Hall PTR*, pp. 36, 2003.